Proceedings of the ASME 2015 Dynamic Systems and Control Conference
DSCC2015
October 28-30, 2015, Columbus, Ohio, USA

DSCC2015-9708

IMPULSE REDIRECTION OF A TETHERED PROJECTILE

Hossein Faraji, Stephanie Veile, Samantha Hemleben, Pavel Zaytsev, Joel Wright, Hans Luchsinger, and Ross L. Hatton
Department of Mechanical, Industrial and Manufacturing Engineering
Oregon State University
Corvallis, Oregon 97331
Emails: farajih@onid.oregonstate.edu, ross.hatton@oregonstate.edu

ABSTRACT

The momentum of a projectile in free flight can be redirected by using a tether to create a "virtual wall" against which it bounces. The direction of this bounce can be controlled actively through braking modulation, or passively through placement of the tether anchor and the orientation of the projectile at impact. In this paper, we explore the space of motions achievable through the latter two methods. In particular, we consider the ways in which holding the tether away from center of mass at different angles can contribute to changes in speed and direction of motion after the bounce.

1 INTRODUCTION

A moving object in free flight can redirect its momentum by pulling on a tether connecting it to the ground or a heavier object. This principle is used by spiders [1] to maneuver while jumping and has been used by astronauts to maneuver during spacewalks [2].

As a step towards the goal of enabling robots to be able to move with this agility, we seek to understand how much and what kind of control authority can be achieved by bouncing against a cable, and in particular by setting up the right pre-bounce initial conditions so that no active feedback is needed during the moment of impact. In this paper, we consider the fundamental case of planar object anchored by a tether attached to either its center of mass or an outboard point, as illustrated in Fig. 1. This tether is slack for most of the motion, then applies a short impulse when the distance between its anchor and attachment point to the body matches its actual length. This impulse can be considered as an impact of the body against a virtual wall that is perpendicular to the tether and passes through the attachment point.

We identify the space of post-bounce motions available by changing the angle of the tether relative to the body's initial motion or the position of the attachment point relative to the center of mass, and in particular consider the ways in which the alignment between the velocity, tether, and offset direction of the attachment point exchange energy between the translational and rotational modes of the body. Along the way, we also identify the accuracy of using an impulse equation that treats the bounce as instantaneous versus modeling the tether as deformable spring. A key result in this paper is the identification of a tether configuration that converts an initial pure translational velocity of the puck into a pure rotational motion after the bounce.

This paper is organized as follows: Section 2 puts our work into the context of previous studies on tethered systems. Section 3 describes the modeling of the system in terms of both the full dynamic equation and an impulse approximation. Section 4 considers several case studies of the system dynamics with different initial conditions. Section 5 describes the experimental results

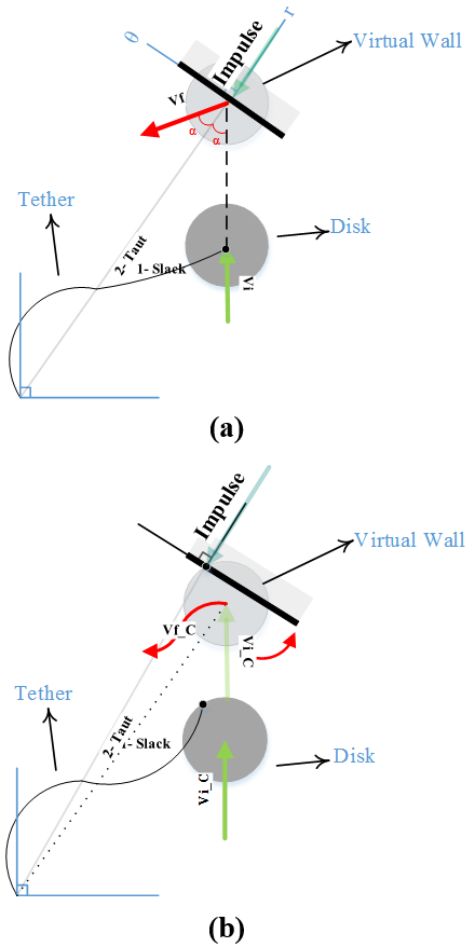

FIGURE 1: BOUNCING A PROJECTILE AGAINST A TETHER (a) ATTACHED TO THE CENTER OF MASS, AND (b) ATTACHED TO THE OUTBOARD FROM THE CENTER OF MASS.

that we implemented on a physical realization of our idealized system. Finally, Section 6 presents a discussion on the relevance of the results and highlights directions for future work.

2 BACKGROUND

Our analysis in this paper draws on prior research efforts regarding casting manipulators, string pendula, and balls bouncing against walls.

2.1 Casting Manipulation

In order for the robots to perform in uncertain and unstable environments, it is crucial to extend their workspace using their mobility. However, mobile robots such as legged and wheeled robot still have difficulty in moving in wasteland, steep slopes, etc. Casting manipulators are robots that can throw an end effector which is attached the robot by a tether. A key aspect of casting manipulation is midair control of the end-effector by applying an impulsive force through the tether that causes the end-effector to approach a desired target [3]. When the moving body is arrested by the tether during the flight, it rebounds. This phenomenon can be thought that there is a virtual wall perpendicular to the string. This idea has been experimented in Kendama game [4]. Also, [5, 6] considered the effects of bouncing with an off-center attached tether, but that they didn't examine the geometry of bounce direction and speed. In this research we utilize the idea of the virtual wall that happens in impact time and will consider the geometry and physics of the moving body with off-center attached tether after the impact.

2.2 String Pendulum

Our system is a special case of a string pendulum, a class of systems in which the element connecting the pendulum bob to the pivot can only provide tension, and acts as a high-stiffness spring when taut. Prior research on these systems mostly has focused on the periodic motion of such pendula, as in [7]. In our work here we focus on the transient response around the slack-taut transition, rather than the long-term dynamics.

2.3 Classic case of a bouncing ball

The dynamics of the system we are considering are very similar to those of a ball bouncing against a wall [8]. When modeled as a point mass, the ball's velocity normal to the wall changes signs while its velocity parallel to the wall is unaffected, so that its angles of incidence and reflectance are the same. For a ball with finite radius, the angle of reflection will in general be different from that of the point mass, as some of the ball's kinetic energy is transferred into or out of its spinning mode [9]. Our tethered-projectile model extends this concept by allowing the bounce point to be inside the perimeter of the moving object, opening up the potential for a wider variety of post-impact behaviors.

3 MODELING OF THE SYSTEM AND COORDINATES

Our model system for this study consists of a puck (a solid disk moving in the plane) anchored to the ground by a stiff, elas-

tic, and massless tether. We consider this system under two conditions. In the first, simpler case, the tether is attached to the puck's center of mass;[1] in the second case the tether is attached to a point outboard from the center of mass. This outboard attachment allows for a variable moment arm between tether's line of action and the center of mass, and thus for different amounts of energy to be transferred between translational and rotational modes at impact.

Fig. 2 illustrates the coordinates we use to model this system, where x and y are the position of the puck with respect to the global reference frame and the puck's initial velocity is in the y direction. The tether is anchored to the origin of the global frame, and is at an angle β with respect to this frame; it has a base length L_0 when it is taut and not stretched. For a tether attached outboard from the puck's center of mass, the line connecting the attachment point and center of mass makes an φ with the direction of motion.

When using an impulse model of the bounce dynamics, as in §3.2, it is useful to transform the system dynamics into a frame whose axes are aligned with or orthogonal to the tether, as illustrated in Fig. 3, and to measure the tether angle with respect to the initial direction of motion, rather than the x axis of the global frame. It is also useful to introduce an "offset angle" α that represents the declination of the line from the tether attachment point to the center of mass, relative to the tether's line of action.

3.1 Full Equations of Motion

The tethered-puck system described above exhibits hybrid dynamics, in that it obeys free-flight equations of motion

$$\ddot{x} = \ddot{y} = \ddot{\varphi} = 0 \tag{1}$$

when the tether is slack, and spring and spring-mass equations of motion

$$m\ddot{x} + k(L - L_0)\cos(\beta) = 0 \tag{2}$$
$$m\ddot{y} + k(L - L_0)\sin(\beta) = 0 \tag{3}$$
$$I\ddot{\varphi} + k(L - L_0)\sin(\beta + \varphi)R = 0 \tag{4}$$

when the tether is taut, where

$$L = \sqrt{(x - R\cos(\varphi))^2 + (y + R\sin(\varphi))^2} \tag{5}$$

[1]The tether is out of the plane of the puck, and so is allowed to intersect with it.

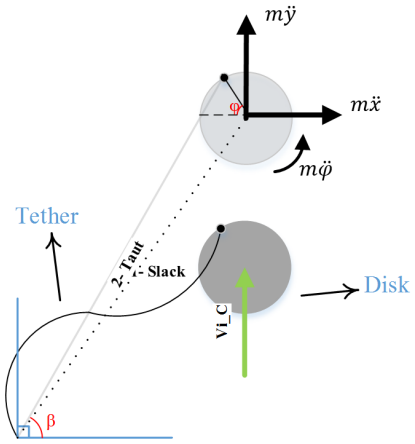

FIGURE 2: COORDINATES OF THE DYNAMIC MODEL.

is the length of the tether,

$$\beta = \arctan\frac{y + R\sin(\varphi)}{x - R\cos(\varphi)} \tag{6}$$

is the angle it makes with the coordinate frame, and R is the distance of its attachment point from the center of mass.

For the motions we consider in this paper, the system starts out in free-flight mode with an initial $\dot{y}$ velocity and a nominal tether length $L < L_0$ (corresponding to a slack tether). It then moves until the slack-taut transition condition of $L = L_0$ is reached, at which time it transitions to the spring-mass dynamics, with the tether stretching to $L > L_0$. It remains in these dynamics until the string returns to its $L = L_0$ neutral length, at which point it returns to free-flight with a new velocity determined by the its final state in the spring mode.

3.2 Impulse Approximation

In many situations involving impacts, the duration of contact is short enough that the forces applied to the moving system can be modeled as an impulse, allowing the final velocity to be determined by conservation of energy and momentum instead of evaluating the full dynamic equations over the contact period. For the puck-tether system, these conservation laws lead to four equalities relating the puck's velocity before and after the bounce:

First, the tether cannot apply any forces perpendicular to itself, so the center-of-mass's momentum (and thus velocity) in

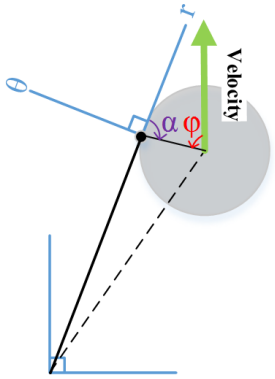

FIGURE 3: EXTRA COORDINATES USEFUL FOR THE IMPULSE MODEL.

that direction is unchanged,

$$v_f^\theta = v_i^\theta. \tag{7}$$

Second, the string applies an impulse $\vec{J} = J\hat{r}$ to the puck, changing the magnitude of its linear momentum along the tether by J,

$$mv_f^r - mv_i^r = J. \tag{8}$$

Third, this linear impulse applies a moment to the system around the center of mass, so that its initial and final angular momenta are related as

$$H_f - H_i = I(\dot{\varphi}_f - \dot{\varphi}_i) = \vec{J} \times \vec{R}, \tag{9}$$

where $\vec{R}$ is the position of the center of mass relative to the attachment point as measured in the tether-aligned coordinates. Fourth and last, a perfectly-elastic tether dissipates no energy during the impact, so the system's initial and final kinetic energies are equal,[2]

$$\frac{1}{2}\left(\vec{v}_f^T m\vec{v}_f + I\dot{\varphi}_f{}^2\right) = \frac{1}{2}\left(\vec{v}_i^T m\vec{v}_i + I\dot{\varphi}_i{}^2\right). \tag{10}$$

Given these relationships, we can solve (7)–(10) as a set of simultaneous equations to extract the final translational and rotational velocities from a set of known pre-impact initial conditions. Note that we need never solve for the impulse J: it acts as a constraint on the dynamic equations that mandates a proportional change in linear and angular momentum, and can be factored out of the system by combining (8) and (9). Additionally, because the exit condition for the impulse equations is that the tether has returned all of its elastic energy to the puck and thus is at $L = L_0$, the equations automatically exclude any solution that would put the tether in compression.

[2]This formula can be generalized to dissipative systems via a coefficient of restitution.

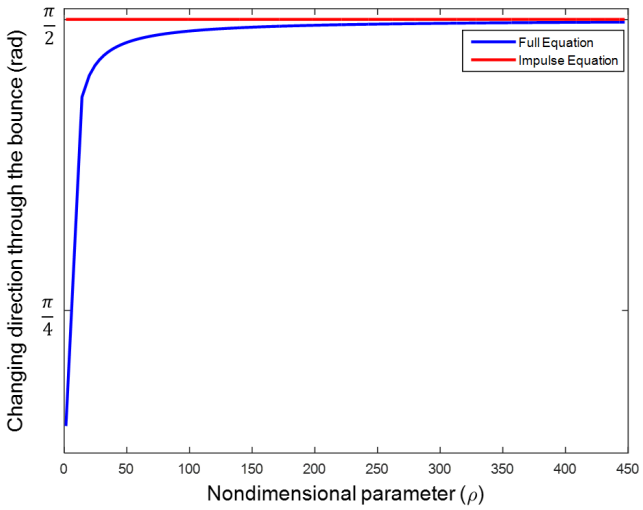

FIGURE 4: THE POST-BOUNCE DIRECTION OF VELOCITY FOR A PUCK WITH A 45° TETHER ATTACHED AT THE CENTER OF MASS, AS A FUNCTION OF THE SYSTEM'S CHARACTERISTIC PARAMETER ρ FROM (11).

3.3 Convergence Study on Impulse Equations

The impulse equations in §3.2 assume that the bounce duration is "small" relative to the time-scale of the system, and in particular that the angle of the tether with respect to the global frame changes very little during the impact. The accuracy of the impulse approximation therefore depends on a non-dimensional parameter ρ that is the ratio of natural frequency of the spring-mass mode of the system and the rate at which the tether is rotating at the start of the impact,

$$\rho = \frac{\omega_n}{\dot{\theta}} = \sqrt{\frac{k}{m}} \cdot \frac{L}{v^\theta}. \tag{11}$$

To validate our use of the impulse equations, we conducted a convergence study between their results and those of the full

equations in (2)–(4), with a 45° tether attached to the center of mass with varying ρ. As illustrated in Fig. 4, the two equations have essentially converged for $\rho > 100$. Our experimental system (described in §5) has $\rho > 850$, well within the region of convergence.

4 EXPLORING BOUNCE DIRECTION WITH THE IMPULSE EQUATIONS

With the impulse model for tether-bounces in hand, we can now explore how the direction in which the system bounces depends on the orientation of the tether, where it is attached to the puck, and the mass distribution of the puck.

When the tether is attached to the center of mass, (7)–(10) have a simple solution: the velocity along the tether is reversed, and the velocity orthogonal to the tether stays the same. As illustrated in Fig. 1, this motion is equivalent to bouncing a point mass off of a virtual wall, with equal angles of incidence and reflection. Such reflections allow for some interesting trajectories, such as a 90° bank shot by placing the tether at 45°, but far more interesting phenomena occur when we consider pucks with outboard tether attachments.

As illustrated in Fig. 5, the bounce direction with an outboard tether is strongly influenced by the relative angle between the tether and the line between the attachment point and the center of mass: aligning these directions produces the same "reflected particle" bounce seen for a tether attached to the center of mass as in Fig. 5a , but the puck bounces by a shallower angle when the tether is at a different angle from the tether attachment as in Fig. 5b. From the standpoint of our momentum equations, this change in bounce direction originates in (9), where the offset angle determines the effective moment arm in the rotational impulse, and thus the proportion of energy that is directed into spinning the puck instead of redirecting its translational velocity.

To further understand the bounce dynamics of this system, we consider how the system's velocity evolves for different offset angles under two conditions: When the tether is at a 45° angle to the initial velocity, and when it is directly inline with the velocity.

4.1 Outboard Attachment With 45° Tether

The bounce directions and relative translational output speed of the puck generated by a half-circle sweep of the attachment point and a fixed[3] tether angle of 45° are plotted in Fig. 6a. As expected, the puck makes a right-angle turn with zero change in speed when there is zero offset between the tether and attachment angles, mimicking a system with the tether attached at the center of mass. Likewise, it experiences the smallest change in direction when the tether is at right angles to the attachment, and thus provides the largest ratio of angular-to-linear impulse; this large ratio means that the system experiences a large rotational acceleration which slackens the tether before the linear momentum is fully redirected. Between these two points, however, we see that the greatest speed change does not occur at this configuration, and in fact corresponds to an offset angle of 45°.

The difference between the minimum-deflection and maximum-deceleration points is an impedance-matching effect-between the system's translational and rotary inertias, in which the impulse applied by the tether most efficiently imparts rotational energy into the system when the moment-arm of the tether force around the center of mass is equal to the puck's radius of gyration, as illustrated in Fig. 7. This condition corresponds to case where the square of the ratio between the magnitudes of its linear and rotational components is equal to the the ratio between the puck's translational and rotational inertia,

$$\left(\frac{JR\sin\alpha}{J}\right)^2 = \frac{I}{m}. \tag{12}$$

For the puck, which has rotational inertia $I = \frac{1}{2}mR^2$, (12) is satisfied when $\sin^2\alpha = \frac{1}{2}$, leading to maximum energy transfer (and thus speed change) at $\alpha = \frac{\pi}{4}$ and $\alpha = \frac{3\pi}{4}$.

The offset angle that results in the maximum change in the puck's speed depends on its mass distribution. If we replace its solid-disk geometry with a thin ring of the same radius, for which $I = mR^2$, then (12) is satisfied for $\sin^2\alpha = 1$. This equation has only a single solution in our domain, $\alpha = \frac{\pi}{2}$. As illustrated in Fig. 6b, this means that the ring's maximum change in velocity is collocated with its minimum deflection.

The evolution of the maximum-deceleration points as a function of I/mR^2 from a pair of solutions evenly distributed about $\alpha = \frac{\pi}{2}$ into a single solution at $\alpha = \frac{\pi}{2}$ with a merge-point at $I = mR^2$ is plotted in Fig. 6c. Note that for pucks whose moment of inertia is greater than $I = mR^2$, (12) has no solution, indicating that the tether's impulse inefficiently applies energy to the rotational mode for any angle; however, the most efficient transfer of energy for these systems still occurs when $\alpha = \frac{\pi}{2}$.

4.2 Tether Inline with Velocity

The effects of offset between the tether and moment arm, and of changing the system's moment of inertia, are even more

[3]On a physical system with a fixed tether length, the tether angle at impact would of course vary with the offset angle. For a sufficiently long tether, however, this change of angle is negligable.

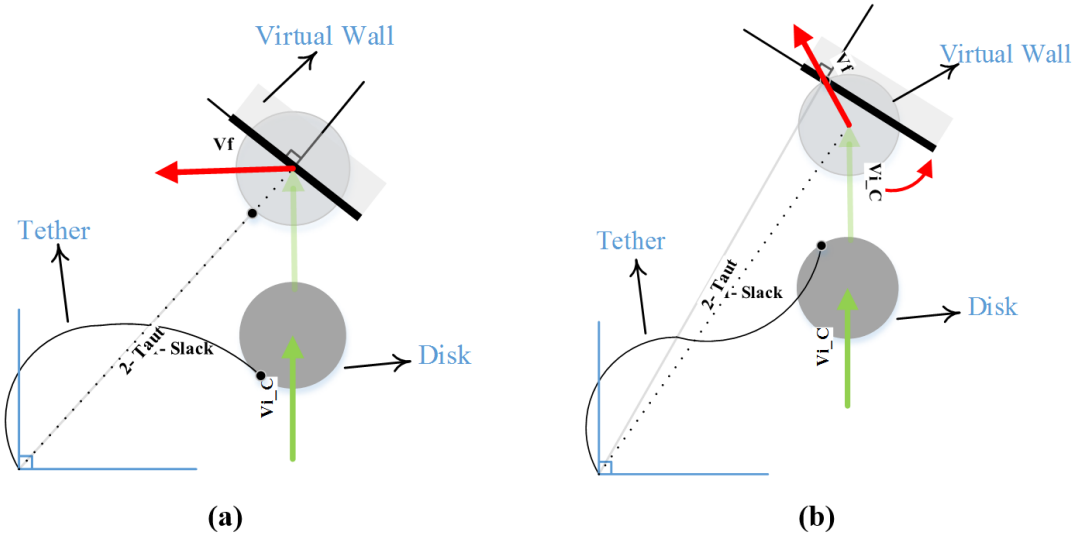

FIGURE 5: BOUNCE DIRECTION WITH OUTBOARD TETHER (A) WHEN THE TETHER'S LINE OF ACTION PASSES THROUGH THE CENTER OF MASS, THE PUCK'S VELOCITY IS REDIRECTED IN THE SAME MANNER AS SEEN WHEN THE TETHER IS ATTACHED TO THE CENTER OF MASS. (B) WHEN THE TETHER'S LINE OF ACTION DOES NOT PASS THROUGH THE CENTER OF MASS, IT REBOUNDS ALONG A SHALLOWER ANGLE.

strongly demonstrated if we consider a tether anchored directly behind the puck. As such a tether is inline with the system's initial linear momentum, it cannot deflect the system at the bounce, and, as illustrated in Fig. 6d, any "change in direction" it produces can only be a complete 180° rebound, and there is a range of offset angles for which there is *no* change in direction: the puck continues moving in its pre-bounce direction, albeit at a slower speed.

An interesting effect appears at the offset angle where the puck transitions from rebounding to carrying on in its original direction: The puck goes to zero translational velocity and instead spins in place. This "deadspin" effect is a special case of the maximum-deceleration point we identified for the 45° tether, where placing the tether's effective moment arm at the puck's radius of gyration now completely transfers its kinetic energy into the rotational mode. The completeness of this energy transfer is enabled by the alignment of the puck's velocity with the tether; in the 45° degree case, the component of the puck's momentum that was orthogonal to the tether represented energy in the system that was unable to interact with the tether.

As was the case for the maximum-deceleration points for the 45° tether, the deadspin points of the 90° tether satisfy the condition $\sin^2\alpha = I/mR^2$, and merge into a single solution for I/mR^2 as illustrated in 6e–f. For moments of inertia above this merge-point, however, there are no dead-spin solutions: the tether's line of action is always inside the radius of gyration, and cannot transfer energy or momentum into the rotational mode efficiently enough to prevent rebound.

5 EXPERIMENTS

In conjunction with our analytical and numerical investigation of tethered-projectile redirection, we also carried out a series of experimental tests on this process. We attached a lightweight tether to a puck on an air hockey table, then used a pendulum-hammer to apply a repeatable initial velocity to the puck. We then tracked the puck's subsequent motion via a high-speed camera (GoPro, HERO3+, 1080p) at 60 frames per second (fps) and extracted its trajectory by processing the video data. Results from two series of these experiments are presented in Figs. 8 and 9.

Our first experiment was to test the bounce direction of a puck with a tether attached to the center of mass for different tether angles. The impulse model predicts that there should be a 2:1 linear relationship between the tether angle and the puck deflection, based on the requirement of equal incident and reflection angles. As shown in Fig. 8, the measured bounce direction closely matched this prediction. The small negative error in the data is most likely a result of energy dissipation in the tether, which would reduce the rebound component of the final velocity and thus the deflection angle.

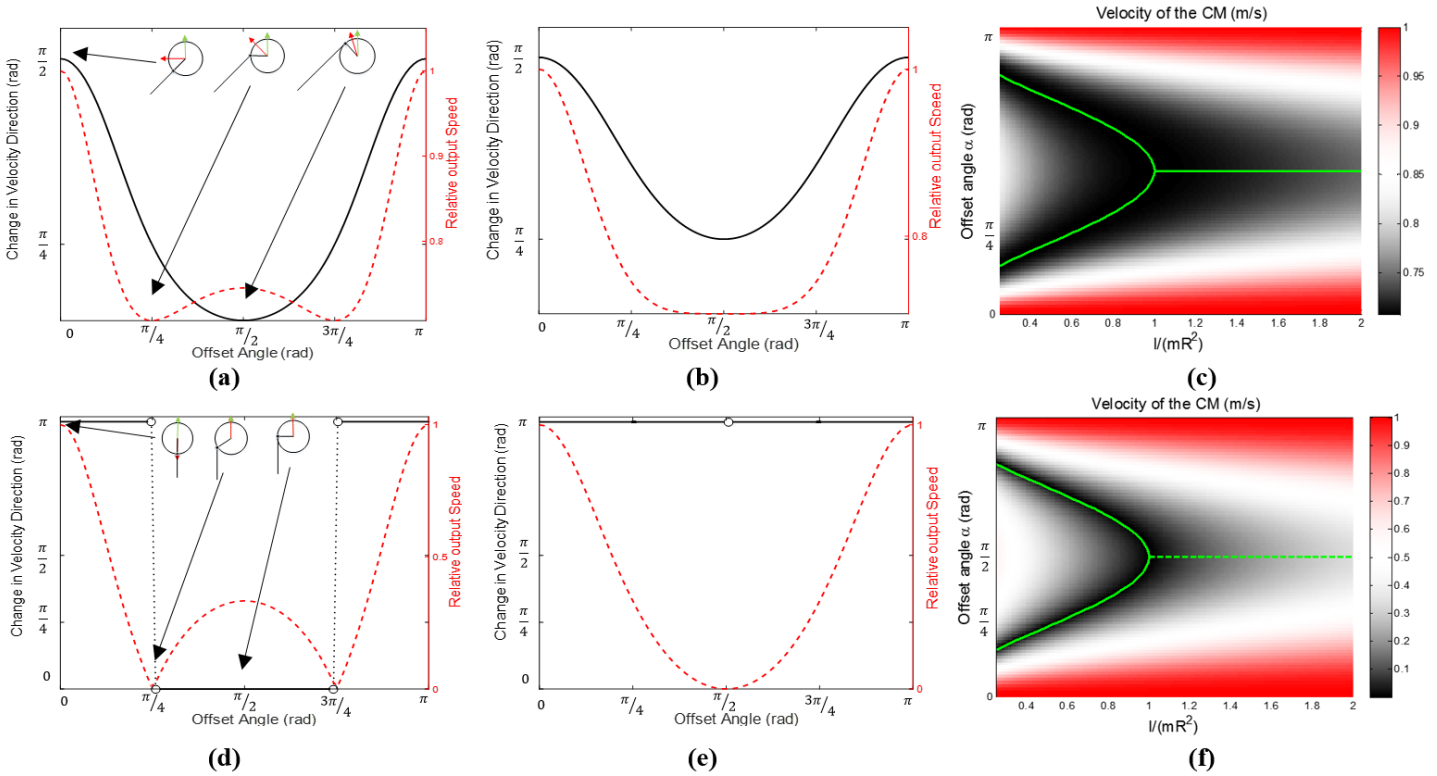

FIGURE 6: BOUNCE DIRECTION AND MAGNITUDE AS A FUNCTION OF TETHER AND OFFSET ANGLE. (a) WITH A 45° TETHER ANGLE, THE PUCK EXPERIENCES MAXIMUM DEFLECTION (CHANGE IN DIRECTION) WHEN THE OFFSET ANGLE IS ZERO, MAXIMUM DECELERATION WHEN THE OFFSET ANGLE IS $\frac{\pi}{4}$ OR $\frac{3\pi}{4}$, AND MINIMUM DEFLECTION WHEN THIS ANGLE IS $\frac{\pi}{2}$. (b) A PUCK THAT IS A RING (INSTEAD OF A SOLID DISK) EXPERIENCES BOTH MAXIMUM DECELERATION AND MINIMUM DEFLECTION AT AN OFFSET ANGLE OF $\frac{\pi}{2}$. (c) FOR INERTIA RATIOS OF $I/mR^2 < 1$, THE MAXIMUM DECELERATION OCCURS WHEN THE TETHER'S LINE OF ACTION IS TANGENT TO THE RADIUS OF GYRATION. THE LOCUS OF SUCH POINTS (WHICH SATISFIES (12)) HAS TWO BRANCHES WHICH MERGE TOGETHER WHEN THE INERTIAL RATIO REACHES UNITY. ABOVE THIS LIMIT, MAXIMUM DECELERATION OCCURS WHEN THE TETHER'S LINE OF ACTION HAS A MAXIMAL MOMENT ARM AROUND THE CENTER OF MASS. (d) WHEN THE TETHER IS ANCHORED DIRECTLY BEHIND THE IMPACT POINT, THE MAXIMUM DECELERATION REMOVES ALL TRANSLATIONAL VELOCITY FROM THE PUCK, LEAVING IT IN A "DEADSPIN." (e) THE TWO DEADSPIN POINTS MERGE TOGETHER FOR A RING. (f) THE DEADSPIN POINTS FOR A 90° TETHER TRACE OUT THE SAME LOCUS AS DID THE MAXIMUM-DECELERATION POINTS OF THE 45° TETHER. NOTE THAT THE MAXIMUM-DECELERATION POINTS FOR INERTIA RATIOS GREATER THAN 1 ARE *NOT* DEADSPINS.

In our second experiment, we observed the motion of the puck when the tether was placed at a nominal angle of 45° to the puck's velocity and the tether was attached outboard to the center of mass and at different angles. The data from this experiment is plotted in Figs. 9, and once again shows a good correlation to the experiments. We attribute the error in this plot to a combination of energy dissipation in the tether and a small rotational disturbance in the initial conditions set by the pendulum hammer and from drag on the slack tether. We correct for the net rotation from these sources by plotting the puck's deflection relative to the actual measured initial angle, but the spin also adds energy to the system that is more difficult to accurately capture and compensate for.

Finally, in the third experiment, we tested the deadspin effect. A challenge in observing this effect is that unless the string is released from the base after the impulse is finished, the puck will bounce a second time after making a half-revolution. To avoid this second bounce, we constructed a dynamically-equivalent system, illustrated in Figs. 10 in which the tether is replaced by an orthogonal wall. The wall is raised slightly to allow the puck to slide beneath it, but to catch against a pin at the puck's "tether attachment point" and provide an equivalent im-

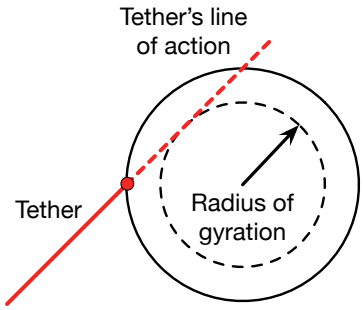

FIGURE 7: THE TETHER IMPULSE MOST EFFICIENTLY TRANSFERS ENERGY INTO THE SYSTEM'S ROTATIONAL MODE WHEN THE TETHER'S LINE OF ACTION IS TANGENT TO THE PUCK'S RADIUS OF GYRATION (THE ROOT-MEAN-SQUARE RADIUS OF ITS MASS ELEMENTS OR, EQUIVALENTLY, THE RADIUS OF A THIN RING WITH THE SAME MOMENT OF INERTIA). THIS ARRANGEMENT BALANCES THE LINEAR INERTIA OF THE PUCK WITH ITS ROTATIONAL INERTIA RELATIVE TO FORCES ACTING ALONG THE TETHER.

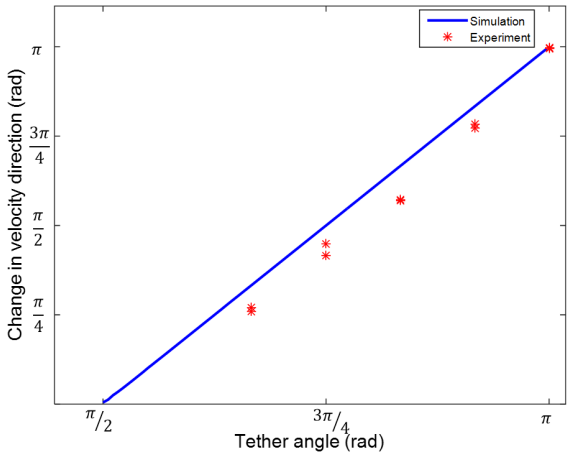

FIGURE 8: COMPARISON OF SIMULATION AND EXPERIMENT IN WHICH THE TETHER IS ATTACHED AT THE CENTER OF MASS AND ITS ANGLE IS VARIED WITH RESPECT TO INITIAL VELOCITY DIRECTION.

pulse. As can be seen from the captured images and the attached video, the puck indeed goes into the deadspin predicted by the model and makes more than a full revolution without leaving the red area at the center of the air table.

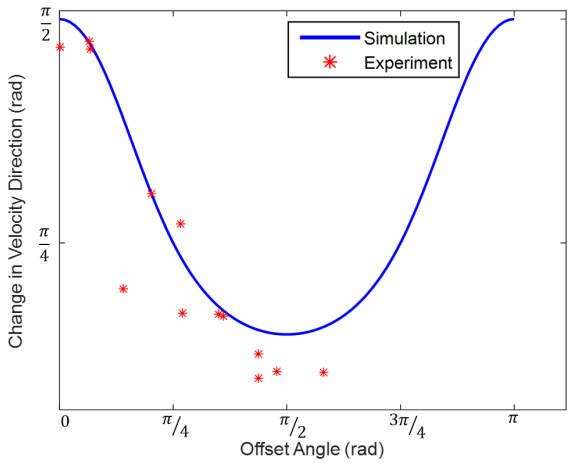

FIGURE 9: COMPARISON OF SIMULATION AND EXPERIMENT IN WHICH THE TETHER ANGLE IS SET AT A 45° ANGLE RELATIVE TO THE PUCK'S INITIAL VELOCITY, AND THE OFFSET ANGLE α IS VARIED.

6 CONCLUSION

In this paper, we investigated the direction in which a moving projectile anchored by a tether will bounce when the tether becomes taut. In doing so, we identified three critical points in the puck's dynamics:

1. The puck is *maximally deflected* when the tether's line of action passes through the center of mass, and so transfers no energy into the rotational mode.
2. The puck is *minimally deflected* when the tether's line of action is at right angles to the line connecting its attachment point to the center of mass. In this configuration, the impulse's moment-to-force ratio is large, and the puck rotates into the tether (causing it to go slack) before it can fully redirect its linear momentum.
3. The puck is *maximally decelerated* when the tether's line of action is tangent to the puck's radius of gyration, and so optimally transfers energy into the rotational mode and out of the translational modes.

In our future work, we aim to build on these results by incorporating the bounce dynamics into a system that can actively change its orientation during flight, e.g., by coupling to a flywheel or other reaction mass. We anticipate that the combination of the bounce and orientation dynamics will lead to the development of mobile systems with novel maneuvering capabilities. We will also be incorporating our bounce analyses into our ongoing work on casting manipulation [10] (interacting with the en-

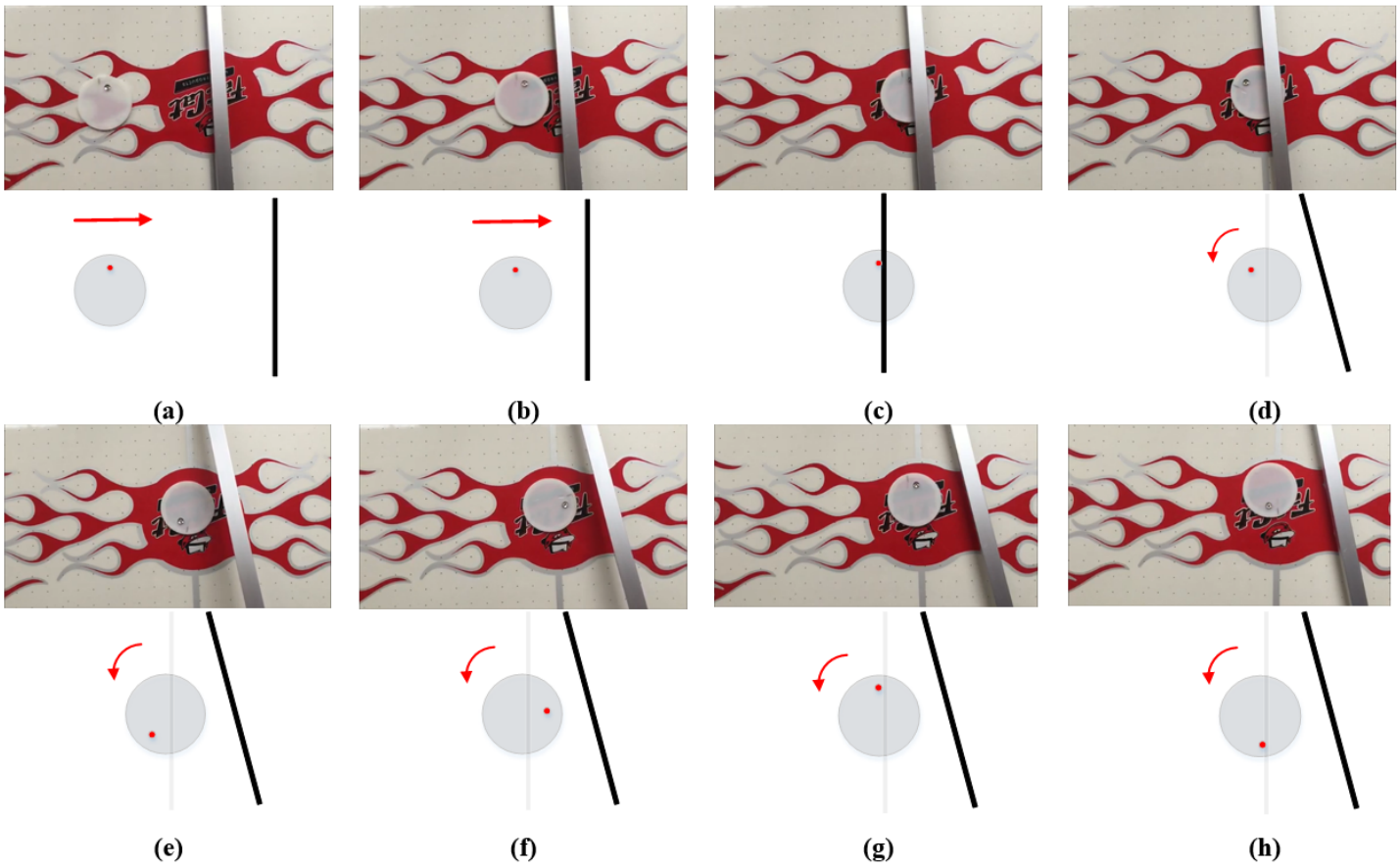

FIGURE 10: EXPERIMENTAL VALIDATION OF THE DEADSPIN EFFECT DESCRIBED IN §4.2. THE PUCK CAN SLIDE UNDER THE BAR, BUT HAS A PIN THAT CAN CATCH ON THE BAR, AND SO IS DYNAMICALLY-EQUIVALENT TO THE TETHERED PUCK. WITH AN INITIAL VELOCITY PERPENDICULAR TO THE WALL AND THE PIN AT THE PUCK'S RADIUS OF GYRATION, THE PUCK GOES INTO A DEADSPIN ON IMPACT AND STOPS AT THE SAME PLACE. WE REMOVE THE BAR AFTER THE INITIAL IMPACT—BETWEEN (C) AND (D)—TO PREVENT THE PUCK FROM EXPERIENCING A SECOND BOUNCE BETWEEN (E) AND (F). NOTE THAT THE CAMERA WAS ANGLED IN THE EXPERIMENT, BUT THE BAR IS SHOWN CORRECTLY IN THE CARTOON AS BEING PERPENDICULAR TO THE VELOCITY DIRECTION.

vironment via an end-weighted tether) and spring-mass legged locomotion [11]. Lastly, we will seek to broaden the scope of our bounce dynamics study, considering effects such as energy dissipation or continuous drag on the tether (both of which are used for maneuvering and orientation-control by some spiders [1]) and the effects on bounce direction from starting with non-zero rotational velocity (as in the case of an astronaut performing emergency maneuvers during a spacewalk by pulling against his safety tether [2]).

ACKNOWLEDGMENT

We would like to thank Lucas Hill, Ramsey Tachella, and Chad Orenberg for their contributions to, and discussions of, this work.

This work was supported in part by the NSF, under REU award CNS 1359480.

REFERENCES

[1] Chen, Y.-K., Liao, C.-P., Tsai, F.-Y., and Chi, K.-J., 2013. "More than a safety line: jump-stabilizing silk of salticids". *Journal of the Royal Society: Interface,* ***10***(87), p. 20130572.

[2] http://history.nasa.gov/apollo204/zorn/white.htm.

[3] Arisumi, H., Yokoi, K., and Komoriya, K., 2008. "Casting manipulation midair control of a gripper by impulsive force". *IEEE Transactions on Robotics,* ***24***(2), Apr., pp. 402–415.

[4] Arisumi, H., Yokoi, K., and Komoriya, K., 2005. "Kendama game by casting manipulator". In 2005 IEEE/RSJ International Conference on Intelligent Robots and Systems, 2005. (IROS 2005), pp. 3187–3194.

[5] Arisumi, H., Yokoi, K., and Komoriya, K. "Casting manipulation (braking control for catching motion)". In IEEE International Conference on Robotics and Automation, 2000. Proceedings. ICRA '00, Vol. 2, pp. 1961–1968 vol.2.

[6] Arisumi, H., and Komoriya, K. "Catching motion of casting manipulation". In 2000 IEEE/RSJ International Conference on Intelligent Robots and Systems, 2000. (IROS 2000). Proceedings, Vol. 3, pp. 2351–2357 vol.3.

[7] Ciocanel, V., and T., W., 2012. "Modeling and numerical simulation of the nonlinear dynamics of the parametrically forced string pendulum". In Society for Industrial and Applied Mathematics 2012.

[8] Cross, R., 1998. "The bounce of the ball". In American Association of Physics Teachers 1998., pp. 222–227.

[9] Cross, R., 2005. "Bounce of a spinning ball near normal incidence". In American Association of Physics Teachers 2005., pp. 914–920.

[10] Hill, L., Woodward, T., Arisumi, H., and Hatton, R., 2015. "Wrapping a target with a tethered projectile". In 2015 IEEE International Conference on Robotics and Automation, pp. 1442–1447.

[11] Abate, A., Hatton, R., and Hurst, J., 2015. "Passive-dynamic leg design for agile robots". In 2015 IEEE International Conference on Robotics and Automation, pp. 4519–4524.